

## Influences of Ethylene-Butylacrylate-Glycidyl Methacrylate on Morphology and Mechanical Properties of Poly(butylene terephthalate)/Polyolefin Elastomer Blends

Li Yang,<sup>1</sup> Hong Chen,<sup>1</sup> Shikui Jia,<sup>1</sup> Xiang Lu,<sup>1</sup> Jintao Huang,<sup>1</sup> Xingxing Yu,<sup>2</sup> Kunhao Ye,<sup>2</sup> Guangjian He,<sup>1</sup> Jinping Qu<sup>1</sup>

<sup>1</sup>National Engineering Laboratory for Plastic Modification and Processing; National Engineering Research Center of Novel Equipment for Polymer Processing; South China University of Technology, Guangzhou, 510640, People's Republic of China

<sup>2</sup>Guangzhou KINGFA Sci. & Tech. Co., Ltd, Guangzhou, 510640, People's Republic of China

Correspondence to: J. Qu (E-mail: jpqu@scut.edu.cn)

**ABSTRACT:** Elastomer ethylene-butylacrylate-glycidyl methacrylate (PTW) containing epoxy groups were chosen as toughening modifier for poly(butylene terephthalate) (PBT)/polyolefin elastomer (POE) blend. The morphology, thermal, and mechanical properties of the PBT/POE/PTW blend were studied. The infrared spectra of the blends proved that small parts of epoxy groups of PTW reacted with carboxylic acid or hydroxyl groups in PBT during melt blending, resulting in a grafted structure which tended to increase the viscosity and interfere with the crystallization process of the blend. The morphology observed by scanning electron microscopy revealed the dispersed POE particles were well distributed and the interaction between POE and PBT increased in the PBT/POE/PTW blends. Mechanical properties showed the addition of PTW could lead to a remarkable increase about 10-times in impact strength with a small reduction in tensile strength of PBT/POE blends. Differential scanning calorimetry results showed with increasing PTW, the crystallization temperature ( $T_c$ ) and crystallinity ( $X_c$ ) decreased while the melting point ( $T_m$ ) slightly increased. Dynamic mechanical thermal analysis spectra indicated that the presence of PTW could improve the compatibility of PBT/POE blends. © 2014 Wiley Periodicals, Inc. *J. Appl. Polym. Sci.* **2014**, *131*, 40660.

**KEYWORDS:** blends; compatibilization; elastomers; grafting

Received 7 December 2013; accepted 27 February 2014

**DOI:** 10.1002/app.40660

### INTRODUCTION

Polymer blending has been one of the most effective and attractive techniques to generate new polymeric materials.<sup>1,2</sup> Polymer blends are important engineering materials with outstanding comprehensive performance by taking advantages of each component. Poly(butylene terephthalate) (PBT) is a semicrystalline plastic with numerous applications, due to its unique property, such as rigidity, and high rates of crystallization.<sup>3,4</sup> However, PBT does not show sufficient toughness, particularly, the high notched impact strength.<sup>5,6</sup> Therefore, to improve fracture toughness, especially impact toughness, the incorporation of rubber or other elastomer is often required.<sup>7-9</sup>

Polyolefin elastomer (POE) is a thermoplastic elastomer with a good processability and superior toughness. Its elastomeric nature has allowed it to be used as an impact modifier for PBT and PP.<sup>10,11</sup> However, simple blends are usually immiscible

which may lead to unsatisfactory mechanical properties. Reactive blending that will improve the miscibility of polymer blends and increase interfacial adhesion between matrix and dispersed phase is a useful way to obtain blends with desirable properties.

Poly(ethylene-butylacrylate-glycidyl methacrylate) (PTW) is a new copolymer containing epoxy groups, which could react preferentially with carboxyl and hydroxyl groups in PBT.<sup>12</sup> The butylacrylate segments could provide satisfactory low temperature properties and compatibility with POE. Therefore, PTW is an attractive impact modifier because of both reactive processing and rubbery toughening.<sup>13,14</sup>

The binary blend of PBT with different contents of POE was studied in this article. Results showed that the effect of POE on the improvement of the notched impact strength was not as obvious as imagined. Aiming at a further improvement of the toughness of PBT/POE blends without significantly compromis-

**Table I.** Components of Different Samples

Component Sample	PBT	POE	PTW
1	100	-	-
2	95	5	-
3	90	10	-
4	80	20	-
5	95	-	5
6	80	20	0.5
7	80	20	1
8	80	20	2
9	80	20	5

ing the other properties, PTW was introduced into the PBT/POE blend as compatibilizer in this study. All of the components were mixed together in a twin-screw extruder and subsequently injection molded. The blends were characterized by dynamic mechanical thermal analysis (DMA), differential scanning calorimetry (DSC), and scanning electron microscopy (SEM). The mechanical properties were measured with tensile, and impact tests and were related to the morphology of the blends.

The main contribution of this article is an achievement of great enhancement on impact strength of PBT/POE blends modified by low priced PTW, which may help broaden the application of PBT in engineering fields. The main reason for this improvement is due to the reactive compatibilization effect of PTW, which had also been proved in this article through following characterization methods.

## EXPERIMENTAL

### Materials

The PBT used in this study was 1200-211M (Yizheng Chemical Fiber Group Corp., China), having a melt flow index (MFI) of 42–49 g/(10 min) (235°C/2.16 kg). POE 8137 (0.864 g/cm<sup>3</sup>), having a MFI of 13 g/(10 min) (190°C/2.16 kg), with a melt temperature of 56°C, was supplied by The Dow Chemical Company. PTW (0.94 g/cm<sup>3</sup>), containing 0.4 wt % grafted glycidyl methacrylate, ethylene acrylate copolymer content >98 wt %, having a MFI of 12 g/(10 min) (190°C/2.16 kg), with a melt temperature at 72°C, was purchased from Dupont Co. Ltd.

### Preparation of the Blends

The PBT (4 h at 120°C), POE, and PTW particulates (4 h at 70°C) were dried before processing in an air oven to avoid possible moisture-degradation reactions. The content of PTW with respect to a 100% PBT/POE blend (80/20) changed from 0 to 5.0 phr. PBT/POE/PTW (80/20/5) represents an 80/20 blend with a PTW content of 5.0 phr. The content of the samples studied in this research are listed in Table I.

The blends, with a fixed ratio of PBT to POE (80/20) and a different content of PTW (0, 0.5, 1, 2, and 5 phr), were prepared in a Berstoff twin-screw extruder (type 25A, L/D ratio 40, screw

diameter 25 mm), at a screw speed of 200 r/min. The temperature profiles of the barrel were 60°C–230°C–250°C–250°C–250°C–250°C–250°C–250°C from the hopper to the die. All the extruded rods were cooled in a water bath immediately, and a pelletizer was used to cut the extrudates for obtaining the blend pellets, and dried in an air oven for 4 h at 120°C. The injection molding was carried out in a plastic injection molding machine (HTB110X/1, China) to obtain tensile and impact specimens for observations. The barrel temperature profiles of the injection molding were 250°C–245°C–245°C–240°C, the injection pressure was 55 MPa, dwell pressure was 45 MPa, and the mold temperature was 50°C. The mixing time was 3 seconds, the dwelling time was 4 seconds, and the cooling time was 10 seconds.

### DSC

The thermal behavior of the blends was studied by DSC using a Netzsch DSC (model 204c, Germany) equipped with a liquid nitrogen-cooling accessory. Specimens were first heated from room temperature to 260°C at 10°C/min, and maintained for 3 min to eliminate thermal history, then cooled to 30°C at the same rate. Then, the cooled samples were also reheated from 30°C to 260°C at a rate of 10°C/min.

### DMA

DMA was performed with a Netzsch DMA242c instrument dynamic mechanical analyzer at a fixed frequency of 10 Hz and oscillation amplitude of 0.15 mm to provide the plots of the loss factor (tan  $\delta$ ) and the storage modulus against the temperature. The scans of the blends were carried out in a three-point bending mode at a constant heating rate of 3°C/min and at a frequency of 10 Hz from 30°C to 170°C, however, the pure PBT was tested at a temperature range from –100°C to 100°C, at the same heating rate and frequency.

### Chemical Structural Analysis

IR spectra of pure PBT and the blends were obtained from an American instrument (Nexus 670, Nicolet Company), which has 0.1–0.005 cm<sup>-1</sup> resolution ratio. Before testing, the specimens were pressed into a film (0.03 mm) by two heated molds at 250°C. Then these samples were measured at 400–4000 cm<sup>-1</sup>.

### SEM

In order to estimate the particle size of the PTW phase dispersed in the PBT matrix and the morphology of the blend, the specimens (4 mm thick) were submerged in liquid nitrogen for approximately 15 min and fractured to expose the internal structure for SEM investigations with a SEM (model HITACHI S-3700N, Japan). The number-average particle diameter ( $d_n$ ) was calculated from a minimum of 200 particles as  $d_n = \frac{\sum n_i d_i}{\sum n_i}$ , where  $n_i$  is the number of particles with a diameter  $d_i$ . To better clarify the brittle–ductile transition of the specimens with different content of PTW in this research, the impact-fractured surfaces were also investigated by SEM. Before testing, all the specimens were gold-sputtered to provide enhanced conductivity.

### Mechanical Properties

The tensile properties were measured with a CMT 4204 universal testing machine (Shenzhen SANS Testing Machine Co., Ltd.,

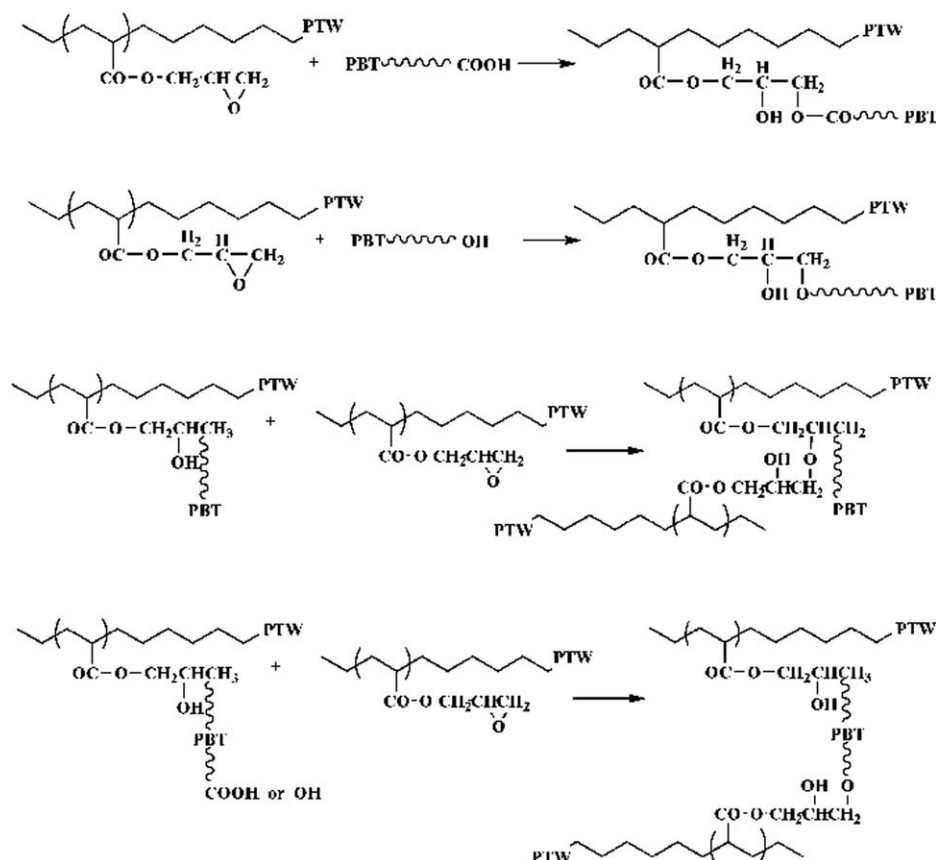


Figure 1. Reactions between PTW and PBT during melt blending.

Shenzhen, China) at a cross-head speed of 50 mm/min according to the GB/T 1040-92 standard. Instron POE2000 pendulum impact tester was used in impact test at room temperature (25°C). For all the mechanical property determination, five or more samples were tested, and then the results were averaged.

#### MFI

MFI was performed with a MTS ZRZ2452 MFI instrument in accordance with ASTM D1238-04 standard. The test temperature and loading points were 230°C and 2.16 kg, respectively. MFI value is determined by the following formula:

$$MI = \frac{m \times 600}{t} \text{ (g/10 min)}$$

where  $m$  is the average mass, and  $t$  is the time required for each cut segment.

## RESULTS AND DISCUSSION

### IR Spectra

PTW used as modifiers to improve toughness of PBT mixing blends had been studied before.<sup>12,15</sup> It is known that the epoxy groups in PTW can easily react with the carboxylic acid or hydroxyl groups in PBT. The major chemical reactions involved in this reactive compatibilized blend system can be expressed by the following reactions in Figure 1.

IR spectra of PBT, PTW, PBT/POE blend, and PBT/POE/PTW blends are shown in Figure 2, the absorption peaks at 911 and 843  $\text{cm}^{-1}$  which are characteristic of the asymmetric stretching

of the epoxy group in PTW are represented.<sup>16–18</sup> To compare the curves of pure PBT and the PBT/POE/PTW blends with

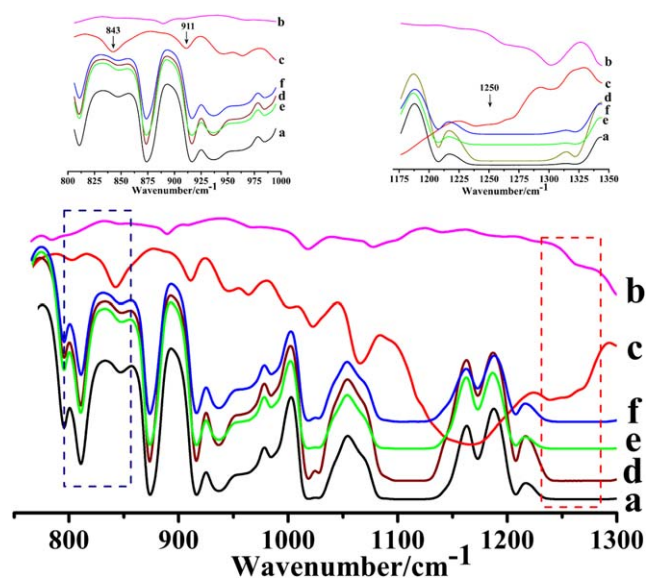
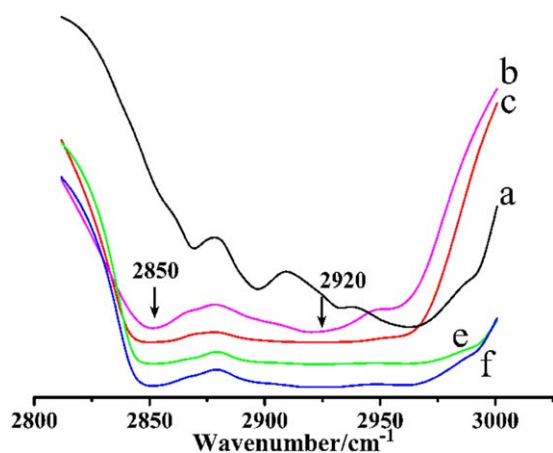


Figure 2. IR spectra of different samples during the fingerprint spectrum: (a) pure PBT, (b) pure POE, (c) pure PTW, (d) PBT/POE (80/20), (e) PBT/POE/PTW (80/20/0.5), and (f) PBT/POE/PTW (80/20/5). [Color figure can be viewed in the online issue, which is available at wileyonlinelibrary.com.]



**Figure 3.** IR spectra of different samples during the functional groups spectrum: (a) pure PTW, (b) pure PBT, (c) PBT/POE/PTW (80/20/0.5), (d) PBT/POE/PTW (80/20/5), and (e) pure POE. [Color figure can be viewed in the online issue, which is available at [wileyonlinelibrary.com](http://wileyonlinelibrary.com).]

PTW, similar peaks at 911 and 843  $\text{cm}^{-1}$  are hardly can be found. Moreover, the symmetrical stretching band of epoxy ring usually absorbs near 1250  $\text{cm}^{-1}$ ,<sup>19,20</sup> which can be found in the curve of pure PTW. However, similar peaks cannot be observed in the curves of the blends. The observed decrease of epoxy groups after melt blending indicates epoxy ring-opening reactions between PTW and PBT occur.

To observe the spectra of POE, PTW, and PBT/POE/PTW blends in Figure 3, we can see each of these curves exhibits two large peaks at 2920 and 2850  $\text{cm}^{-1}$ . This indicates the amount

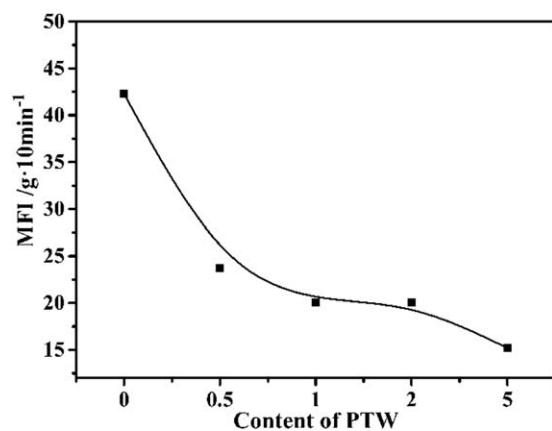


**Figure 4.** The MFI as a function of PTW content in the PBT/POE (80/20) blends.

of  $-\text{CH}_2$  group is far more than that of  $-\text{CH}_3$ .<sup>21</sup> This may be due to the long-chain structure in POE and PTW, and the similar long-chain structure implies that PTW is compatible with POE. All the analysis from IR spectra leads to the point that the presence of PTW has a reactive compatibilizing effect on the blends.

#### MFI

The MFI values of the each sample are shown in Figure 4. The MFI of pure PBT is 47.5 g/10 min. As we can see, for the PBT/POE/PTW blends, the MFI decreased with the addition of PTW, which implied an increase of the viscosity of the blends. The change of MFI indicates a weakening of the mobility of the

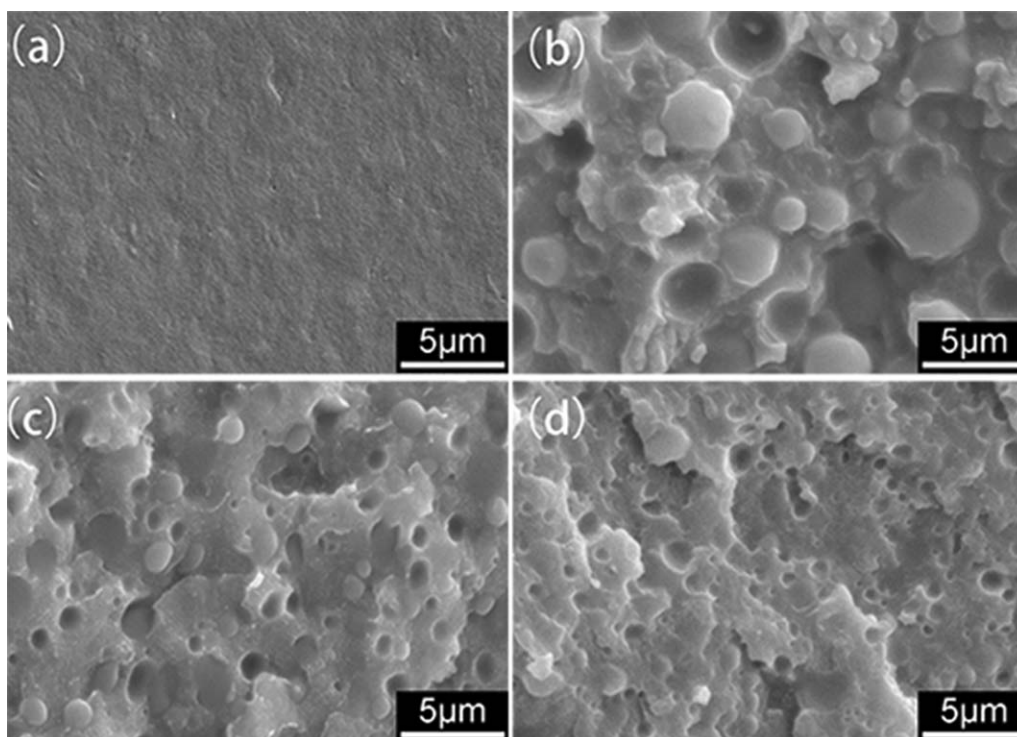


**Figure 5.** Morphology of the cryo-fractured surfaces: (a) pure PBT, (b) PBT/POE (80/20), (c) PBT/POE/PTW (80/20/0.5), and (d) PBT/POE/PTW (80/20/5).

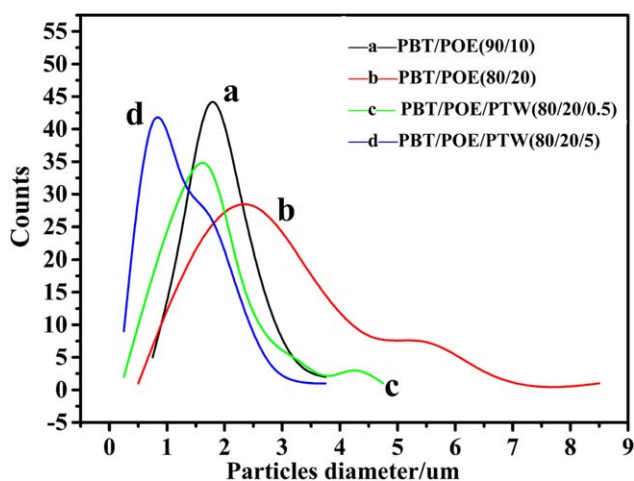


**Figure 6.** The distribution curves of POE size in the blends with and without adding PTW: (a) PBT/POE (90/10), (b) PBT/POE (80/20), (c) PBT/POE/PTW (80/20/0.5), and (d) PBT/POE/PTW (80/20/5). [Color figure can be viewed in the online issue, which is available at [wileyonlinelibrary.com](http://wileyonlinelibrary.com).]

molecule chains, which give direct evidence about the grafting reactions between PBT and PTW.

### Morphology

The SEM observations on the cryo-fractured surfaces of PBT/POE (80/20), PBT/POE/PTW (80/20/0.5), and PBT/POE/PTW (80/20/5) blends are shown in Figure 5(a–d). Clearly, as shown in Figure 5(b), the binary blend has a poor dispersion of POE particles. The interface of the phases is smooth, and many POE

particles separated from the PBT matrix leaving empty holes. This indicates weak interaction and immiscibility between PBT and POE, which may result in poor impact strength. However, when adding PTW to the blend, a remarkable change took place on the phase state of dispersed POE, the particles of POE became evenly distributed, and the interface became more obscure. The distribution curves of POE size in the blends with and without adding PTW are shown in Figure 6, with the addition of PTW, the number average size of POE particles decreased and the distribution became more uniform. The graft copolymer could decrease the interfacial energy and yield smaller particle size, which suggests a better interaction between POE and PBT, indicating that elastomer component of PTW could effectively compatibilize PBT/POE/PTW blend and lead to a phase mixing between the components. These results are consistent with the IR spectra, and may help to explain the improvement on mechanical properties of the blend in the next part.

Figure 7(a–d) shows the impact-fractured surfaces of pure PBT, PBT/POE (80/20), PBT/POE/PTW (80/20/0.5), and PBT/POE/PTW (80/20/5), respectively. The smooth surface from Figure 7(a) indicates a brittle fracture of pure PBT. For the PBT/POE (80/20) blend, a clear interface of the empty holes left by POE and little threads from the deformation of POE can be observed in Figure 7(b), this can be due to the immiscibility between POE and PBT. However, when adding PTW to the blends, dramatic changes can be found on the surface morphologies. With the presence of PTW, no dispersed particles can be found but threads of highly deformed matrix can be observed, which could be due to the interphase chemical reaction of PTW and PBT.

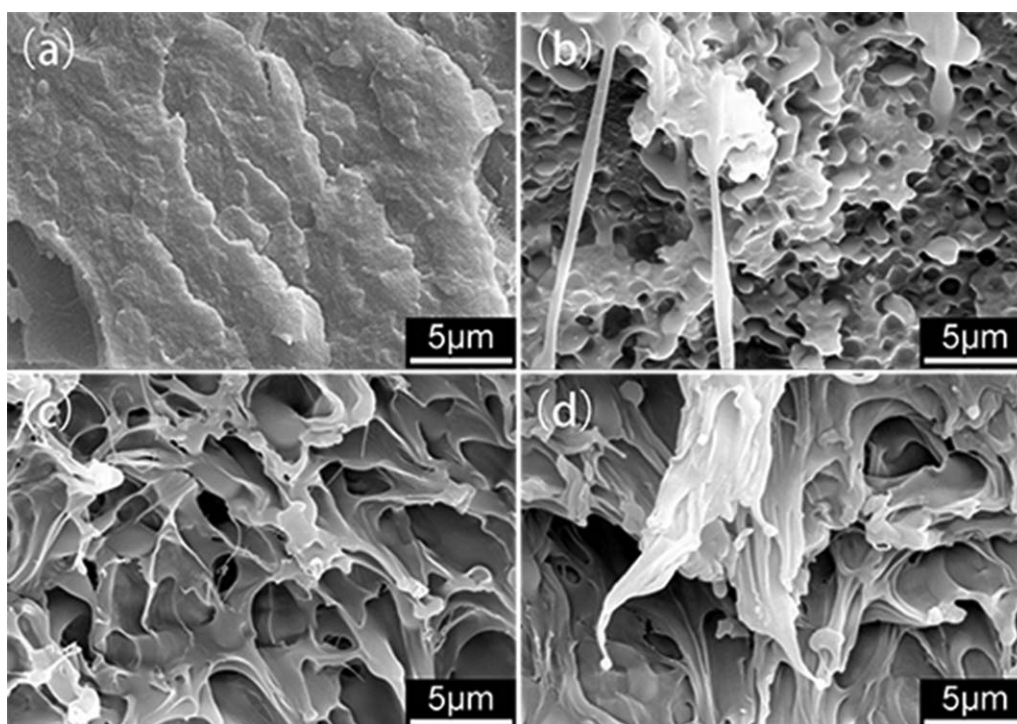


**Figure 7.** Morphology of the impact-fractured surfaces at room temperature: (a) pure PBT, (b) PBT/POE (80/20), (c) PBT/POE/PTW (80/20/0.5), and (d) PBT/POE/PTW (80/20/5).

**Table II.** Tensile Strength and Notched Impact Strength of PBT and Blends

Sample	PBT	PBT/POE			PBT/PTW 95/5	PBT/POE/PTW			
		95/5	90/10	80/20		80/20/0.5	80/20/1	80/20/2	80/20/5
Tensile strength (MPa)	56.83	50.68	46.09	35.51	45.08	33.83	32.74	30.93	29.96
Notched impact strength(kJ/m <sup>2</sup> )	4.92	6.77	6.47	6.18	5.52	25.00	44.48	50.16	50.90

When adding PTW to 5 phr, the threads become denser, which indicates an improvement of interaction between the components.

### Mechanical Properties

The tensile strength and notched impact strength of different samples are listed in Table II. In Figure 8, the tensile strength and notched impact strength of PBT/POE blends with varied POE content are presented. With increasing POE content, the tensile strength decreases from 56.8 to 23.6 MPa. The notched impact strength increased slightly as the POE content approached 5 phr, further increasing POE content to 25 phr brings a small decrease on the impact strength, which may be due to the partial immiscibility between the components.

Figure 9 shows the changes in notched impact strength and tensile strength with variation in weight ratio of the PTW content at the same matrix blends comprised 80 phr PBT and 20 phr POE by weight. When the PTW content was 2 phr, there is a marked increase in impact strength by approximately 10-times over that of PBT/POE blends from 5.9 to 50.2 kJ/m<sup>2</sup>, a super tough PBT/POE/PTW blend obtained. Over a PTW content of 2 phr, the notched impact strength had a slight increase. The tensile strength decreases from 35.2 to 30.1 MPa when the content of PTW increases, the reason for the slight decrease is assigned to the generation of the grafted structure as mentioned in Figure 1. By introducing PTW to the blends, a significant improvement of impact strength is obtained without compromising the tensile properties.

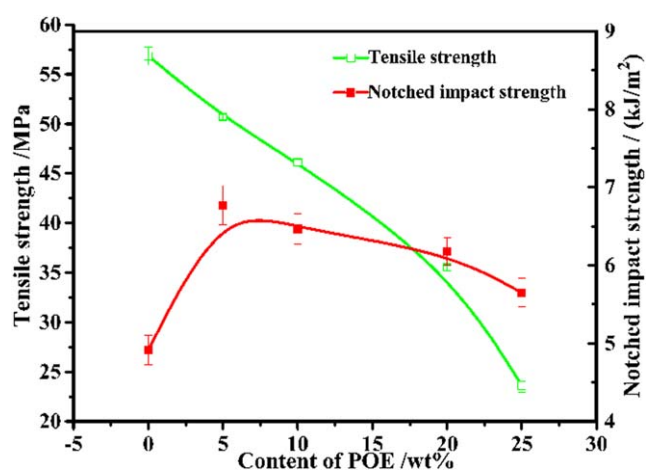


**Figure 8.** The tensile and notched impact strength of PBT/POE blends versus POE content. [Color figure can be viewed in the online issue, which is available at [wileyonlinelibrary.com](http://wileyonlinelibrary.com).]

### DSC Analysis

The crystallization and melting behavior of PBT/POE and PBT/POE/PTW blends are studied by DSC. The cooling thermograms curves are shown in Figure 10. The addition of PTW to PBT/POE decreased the crystallization temperature ( $T_c$ ) of the blends. This may be due to the fact that grafting disrupts the crystallization process of PBT slightly.

From the melting curves in Figure 11, we can see that pure PBT and the blends all exhibit one main melting peak with a minor peak, which is a well-known feature of PBT.<sup>22–24</sup> The first small peak could be attributed to the partial melting of the original less perfect crystals which are results of the fast crystallization rate of PBT.<sup>25</sup> The main melting peak corresponds to the recrystallized crystallites could be attributed to the secondary infilling crystallization during heating.<sup>26–29</sup> To study the first melting peak of PBT and the blends, we can see the first melting point ( $T_{m1}$ ) and second melt temperature ( $T_{m2}$ ) all increase slightly with the addition of PTW. The reason for this is that epoxy groups in PTW have reacted with the carboxylic acid or hydroxyl groups of PBT, resulted in a PTW-graft-PBT structure which is a ternary component that resides at the interface of PBT and POE. The grafting structure decreases mobility of the two phases, which explains the blend is hard to melt.

Table III shows the crystallization temperature ( $T_c$ ), first melt temperature ( $T_{m1}$ ), second melt temperature ( $T_{m2}$ ), melting enthalpy ( $\Delta H_m$ ), and crystallinity percent ( $X_c$ ) of pure PBT and

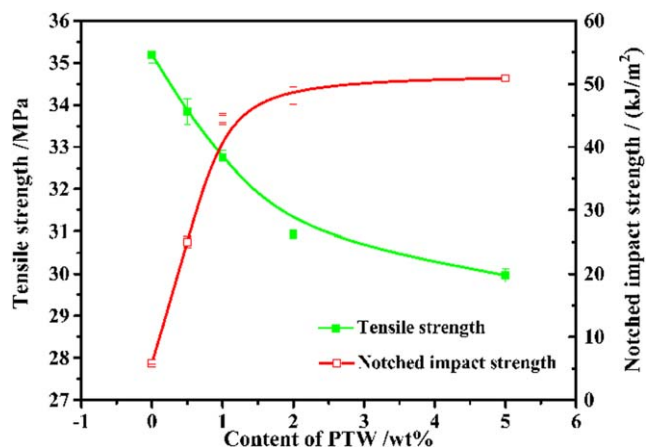


**Figure 9.** The tensile and notched impact strength with variation in weight ratio of the PTW content in the same matrix blends of PBT/POE (80/20). [Color figure can be viewed in the online issue, which is available at [wileyonlinelibrary.com](http://wileyonlinelibrary.com).]

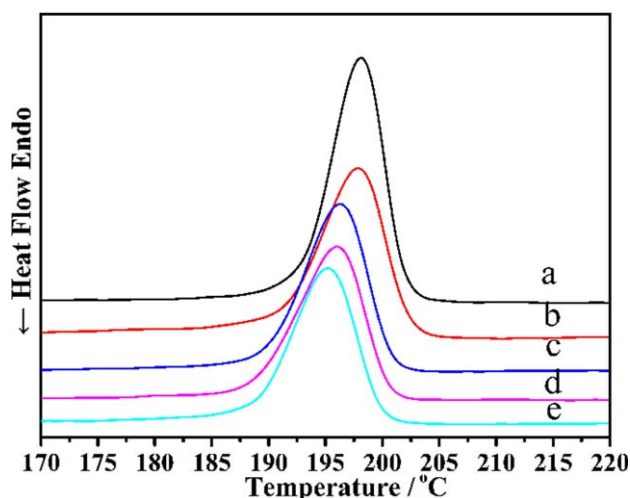


**Figure 10.** DSC cooling thermograms curves of pure PBT and the blends: (a) pure PBT, (b) PBT/POE (80/20), (c) PBT/POE/PTW (80/20/0.5), (d) PBT/POE/PTW (80/20/1), and (e) PBT/POE/PTW (80/20/5). [Color figure can be viewed in the online issue, which is available at [wileyonlinelibrary.com](http://wileyonlinelibrary.com).]

the blends. The  $X_c$  of pure PBT and the blends were determined by eqs. (1) and (2), respectively.<sup>30</sup>

$$X_c = \frac{\Delta H_m}{\Delta H_m^0} \times 100\% \quad (1)$$

$$X_c = \frac{\Delta H_m}{\Delta H_m^0(1 - W_f)} \times 100\% \quad (2)$$

The presence of PTW will inevitably decrease the mobility of PBT chains and interfere with the crystallization process of PBT. From Table III, we can see the melt enthalpy ( $\Delta H_m$ ) and crystallinity ( $X_c$ ) of PBT decreases with increasing PTW content. The decrease of crystallinity may be the partial reason for the increase of impact strength.

### DMA Analysis

DMA data for blends may provide information about glass transition temperatures of components to give better observation on the phase structure and interphase mixing of the blends.<sup>32–34</sup> Plots of loss factor ( $\tan \delta$ ) as a function of temperature for PBT, PBT/POE, and PBT/POE/PTW blends are given in Figure 12. Over the experimental temperature range, PBT exhibited one glass transition temperature at 72°C. Two transition temperatures ( $T_{g1}$  and  $T_{g2}$ ) were observed for

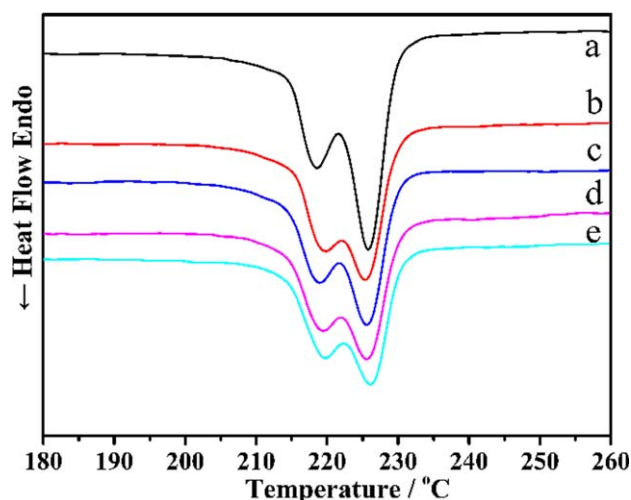


**Figure 11.** DSC heating thermograms curves of pure PBT and the blends: (a) pure PBT, (b) PBT/POE (80/20), (c) PBT/POE/PTW (80/20/0.5), (d) PBT/POE/PTW (80/20/1), and (e) PBT/POE/PTW (80/20/5). [Color figure can be viewed in the online issue, which is available at [wileyonlinelibrary.com](http://wileyonlinelibrary.com).]

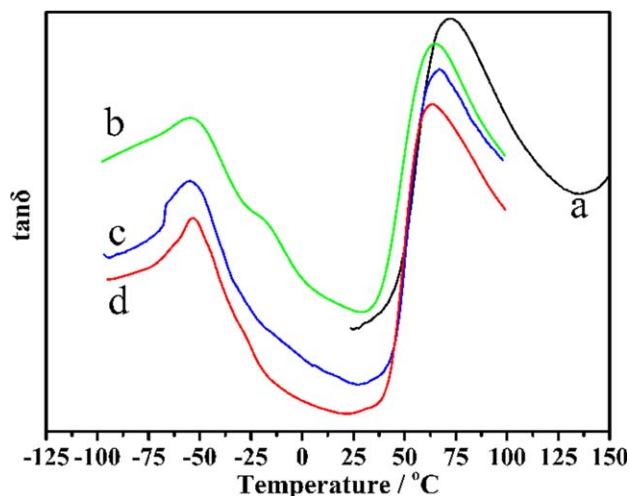
PBT/POE blend, the sharp dynamic mechanical damping peak at approximately 65°C is a result of the glass transition of PBT component, and the broad peak at approximately -55°C is associated with the glass transition temperature relaxation of the POE component in the blend. When adding PTW to a content of 5 phr, it is easy to see that the high peak represents a PBT component shifts to 63°C, while the peak corresponds to a POE component increases to -53°C. Two peaks of PBT and POE have the tendency to move closer when modified by PTW. The glass transition peak of PTW (mostly at -30°C)<sup>35</sup> could not be identified due to their low intensity. These results indicate that the presence of PTW may lead to an increase of compatibility of the blends, which is in agreement with SEM observations.

Figure 13 illustrates the temperature dependence of the storage modulus ( $E'$ ) of pure PBT, PBT/POE and PBT/POE/PTW blends. As we can see, the  $E'$  of PBT/POE blend decreases to 1750 MPa, compared with 2250 MPa of pure PBT. This can be attributed to the flexible chains of POE. With the addition of elastomer PTW to 0.5 phr, the  $E'$  decreases from 1750 to 1300 MPa, which also can be attributed to the introduction of soft segments of PTW. However, when adding PTW to a content of 5 phr, the  $E'$  only decreased by 3.85%. This can be due to the

**Table III.** DSC Data for Pure PBT and Blends

Sample	$T_c$ (°C)	$T_{m1}$ (°C)	$T_{m2}$ (°C)	$\Delta H_m$ (J/g)	$X_c$ (%)
PBT	198.2	218.5	225.7	51.33	36.15
PBT/POE (80/20)	197.9	219.9	225.3	39.62	34.88
PBT/POE/PTW (80/20/0.5)	196.2	218.9	225.7	38.61	34.20
PBT/POE/PTW (80/20/1)	196.0	219.5	225.5	37.33	33.28
PBT/POE/PTW (80/20/5)	195.2	219.7	226.1	35.2	33.05

$T_c$ , crystallization temperature;  $T_{m1}$ , first melt temperature;  $T_{m2}$ , second melt temperature;  $\Delta H_m$ , total melt exotherm of the heating;  $X_c$ , total crystallinity of PBT. The enthalpy value for 100% crystalline PBT used was 142 J/g.<sup>31</sup>



**Figure 12.** Loss factor ( $\tan \delta$ ) versus temperature of pure PBT and the blends: (a) pure PBT, (b) PBT/POE (80/20), (c) PBT/POE/PTW (80/20/0.5), and (d) PBT/POE/PTW (80/20/5). [Color figure can be viewed in the online issue, which is available at [wileyonlinelibrary.com](http://wileyonlinelibrary.com).]

fact PTW-graft-PBT is a ternary component that resides at the interface of PBT and POE. That would explain the large decrease in modulus with 0.5 phr PTW addition. Increasing PTW content would not further change the modulus that much.

## CONCLUSIONS

The multifunctional elastomer PTW is an efficient reactive compatibilizer for PBT/POE blend. The notched impact strength did not significantly improve in PBT/POE blend, however, by adding PTW, a significant improvement of the impact strength was achieved. A super-tough PBT/POE blend was obtained with 5 phr of PTW. The IR observation showed that the terminal epoxy groups in PTW could react with carboxylic acid or hydroxyl groups in PBT which is the main reason for the

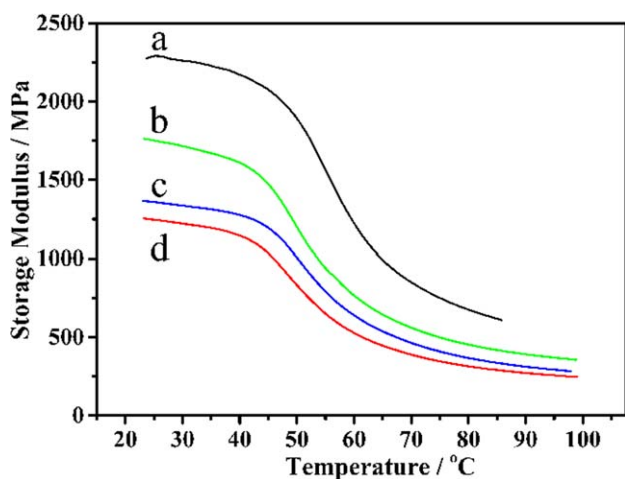


**Figure 13.** Storage modulus ( $E'$ ) versus temperature of pure PBT and the blends: (a) pure PBT, (b) PBT/POE (80/20), (c) PBT/POE/PTW (80/20/0.5), and (d) PBT/POE/PTW (80/20/5). [Color figure can be viewed in the online issue, which is available at [wileyonlinelibrary.com](http://wileyonlinelibrary.com).]

decrease of MFI of the blends. The PTW has a similar long-chain structure as POE, the addition of PTW could result in an enhancement on compatibility of the components. Observations on the cryo-fractured and impact-fractured surfaces showed that PTW improved the interaction and aggravated phase mixing between the matrix and dispersed phase. DSC analysis indicated that PTW-graft-PBT structure will inevitably disrupt crystallization process of PBT, leading to a lower crystallization temperature and crystallinity percent of PBT. The loss factor ( $\tan \delta$ ) analysis indicated that PTW improved the compatibility of PBT and POE. The storage modulus ( $E'$ ) plots also gave indirect proof of the grafting reaction.

## ACKNOWLEDGMENTS

The authors wish to acknowledge Guangzhou KINGFA Sci. & Tech. Co., Ltd., the National Nature Science Foundation of China (Grant 50973035, 51073061, 51373058, and 21174044), National Key Technology R&D Program of China (Grant 2011BAE15B02 and 2009BAI84B06), the Fundamental Research Funds for the Central Universities (NO. 2012ZM0047), Program for New Century Excellent Talents in University (No.NCET-11-0152), Pearl River Talent Fund for Young Sci-Tech Researchers of Guangzhou City (No.2011J2200058), 973 Program (No.2012CB025902) and National Natural Science Foundation of China-Guangdong Joint Foundation Project (U1201242) for the financial supports. Thanks for Miss. Chen (Hong Chen) performed mechanical properties test, Mr. Ye (Kunhao Ye), and Mr. Yu (Xingxing Yu) provide the equipments for processing, Dr. Lu (Xiang Lu) and Dr. Huang (Jintao Huang) performed DMA test, Prof. Qu (Jinping Qu) and Dr. He (Guangjian He) supervise and give guidance on this article, Dr. Jia (Shikui Jia) revised the article.

## REFERENCES

1. Utracki, L. A. *Polymer Alloys and Blends: Thermo-dynamics and Rheology*; Oxford University Press: New York, **1990**.
2. Paul, D. R.; Newman, S., Eds. *Polymer Blends*; Academic: New York, **1978**; Vols. I and II.
3. Rose, P. J.; Mark, H. F.; Bikales, N. M.; Overberger, C. G.; Menges, G.; Kroschwitz, J. I. *Encyclopedia of Polymer Science and Engineering*; 2nd ed.; Wiley Interscience: New York, **1987**; Vol. 7.
4. Olabisi, O., Ed. *Handbook of Thermoplastic*; Marcel Dekker: New York, **1997**; Chapter 20.
5. Kroschwitz, J. I., Ed. *Concise Encyclopedia of Polymer Science and Technology*; Wiley: New York, **1990**.
6. Paul, D. R.; Bucknall, C. B., Eds. *Polymer Blends*; Wiley: New York, **2000**; Vol. 1, pp 95–97.
7. Arostegui, A.; Gaztelumendi, M.; Nazabal, J. *Polymer* **2001**, *42*, 23.
8. Wang, X. H.; Zhang, H. X.; Wang, Z. G.; Jiang, B. Z. *Polymer* **1997**, *38*, 7.
9. Vongpanish, P.; Bhowmick, A. K.; Inoue, T. *Plast. Rubber. Compos. Proc. Appl.* **1994**, *21*, 109.
10. Tai, H. W.; Jin, R. G.; Zhang, L. C. *J. Hebei Univ. Technol. (in Chinese)* **1999**, *28*, 2.



11. Yin, L.; Shi, D.; Liu, Y.; Yin, J. *Polym. Int.* **2009**, *58*, 8.
12. Zhang, C.; Dai, G. *J. Mater. Sci.* **2007**, *42*, 24.
13. Zhang, C.; Shi, Y. H.; Dai, G. C. *J. East China Univ. Sci. Technol. (Natural Science Edition) (in Chinese)* **2008**, *34*, 3.
14. Bai, H. Y.; Liu, X. Y.; Zhang, Y.; Zhang, Y. X. *E-Polymers* **2010**, *10*, 1162.
15. Bai, H. Y.; Zhang, Y.; Zhang, Y. X.; Zhang, X. F.; Zhou, W. *J. Appl. Polym. Sci.* **2006**, *101*, 1.
16. Martin, P.; Devaux, J.; Legras, R.; Van Gurp, M.; Van Duin, M. *Polymer* **2001**, *42*, 6.
17. Tsai, C. H.; Chang, F. C. *J. Appl. Polym. Sci.* **1996**, *61*, 2.
18. Yang, F. X.; Du, R. N.; Luo, F.; Zhang, X. L.; Yang, J. H.; Fu, Q.; Zhang, Q. *Chem. J. Chin. Univ. (in Chinese)* **2010**, *31*, 1.
19. Carturan, S.; Quaranta, A.; Maggioni, G.; Vomiero, A.; Ceccato, R.; Della Mea, G. *J. Sol-gel. Sci. Technol.* **2003**, *26*(1-3), 931.
20. Vijayanand, P. S.; Radhakrishnan, S.; Arun Prasath, R.; Nanjundan, S. *Eur. Polym. J.* **2002**, *38*, 7.
21. Porter, M. D.; Bright, T. B.; Allara, D. L.; Chidsey, C. E. *J. Am. Chem. Soc.* **1987**, *109*, 12.
22. Yang, J.; Shi, D.; Yao, Z.; Xin, Z.; Yin, J. *J. Appl. Polym. Sci.* **2002**, *84*, 5.
23. Huang, J. W.; Wen, Y. L.; Kang, C. C.; Yeh, M. Y.; Wen, S. B. *J. Appl. Polym. Sci.* **2008**, *109*, 5.
24. Chen, H. L.; Hwang, J. C.; Chen, C. C.; Wang, R. C.; Fang, D. M.; Tsai, M. J. *Polymer* **1997**, *38*, 11.
25. Huang, C. C.; Chang, F. C. *Polymer* **1997**, *38*, 9.
26. Cheng, S. Z. D.; Pan, R.; Wunderlich, B. *Macromol. Chem.* **1988**, *189*, 2443.
27. Yeh, J. T.; Runt, J. *J. Polym. Sci. Polym. Phys.* **1989**, *27*, 7.
28. Nichols, M. E.; Robertson, R. E. *J. Polym. Sci. Polym. Phys.* **1992**, *30*, 7.
29. Kim, J.; Nichols, M. E.; Robertson, R. E. *J. Polym. Sci. Polym. Phys.* **1994**, *32*, 5.
30. Durmus, A.; Ercan, N.; Soyubol, G.; Deligöz, H.; Kaşgöz, A. *Polym. Compos.* **2010**, *31*, 6.
31. Larocca, N. M.; Hage Jr, E.; Pessan, L. A. *Polymer* **2004**, *45*, 15.
32. Yang, H.; Lai, M.; Liu, W.; Sun, C.; Liu, J. *J. Appl. Polym. Sci.* **2002**, *85*, 12.
33. Avramova, N. *Polymer* **1995**, *36*, 4.
34. Aoki, Y.; Li, L.; Amari, T.; Nishimura, K.; Arashiro, Y. *Macromolecules* **1999**, *32*, 6.
35. Bai, H. Y.; Zhang, Y.; Zhang, Y. X.; Zhang, X. F.; Zhou, W. *Polym. Test.* **2005**, *24*, 2.